academicJournals

Vol. 7(10), pp. 139-152, December 2015
DOI: 10.5897/IJWREE2014.0616
Article Number: D15761256522
ISSN 2141-6613

http://www.academicjournals.org/IJWREE

International Journal of Water Resources and Environmental Engineering

Full Length Research Paper

Modeling of contaminant transport in 10th of Ramadan City Area, East Delta, Egypt

S. Khalaf[1*] and Mohamed Ibrahim Gad[2]

[1]Irrigation and Hydraulics Department, Faculty of Engineering, Mansoura University, Egypt.
[2]Hydrology Department, Desert Research Center, Cairo, Egypt.

Received 29 September, 2015; Accepted 11 November, 2015

The establishment of new communities and land reclamation projects in the Egyptian desert areas is one of the most important national targets. One of these areas is the 10th of Ramadan city. The main goal of the study is concerned with delineation of groundwater contaminants plume in the future. The results show that; the ions concentrations of most samples from the oxidation ponds resources contain concentrations of Al3+, Cr2+, Fe2+, Ni2+ and Sr2+ exceeding the acceptable limit of WHO (1996) standards. Also, most of the groundwater samples are polluted with Al3+ and Fe2+ and Sr2+ ions. The infiltration from the oxidation ponds and expansion of reclaimed lands irrigated with wastewater reflect critical environmental hazards. The results of the groundwater flow and transport simulation reveal contamination plume expansion. It will travel 1.8, 2.1 and 2.3 km due NE direction after for Al3+, Fe2+ and Sr2+contaminants respectively. It is strongly recommended that wastes from oxidation ponds must not be used in irrigation without tertiary treatment. The oxidation ponds to minimize the pollution of groundwater with heavy metals is highly recommended.

Key words: Hydrogeology, heavy metals, MODFLOW, contaminant transport simulation, 10th of Ramadan City.

INTRODUCTION

In Egypt, great efforts have been done to increase the land reclamation. During the last sixty years, heavy investments have been devoted to turn territories of the unproductive desert into green productive areas, to serve the highly increasing population. Priorities of land reclamation are given to the west and east Nile Delta regions due to the presence of high potential groundwater aquifers of quality and wide plains with deep sandy soil. As a result, the percolation of waste water from domestic industrial or agricultural activities to groundwater depends on the load and behavior of the contaminants as well as geological and hydrogeological factors that control the flow and dispersion of the contaminants. The 10th of Ramadan city is one of the settlements that are constructed on the peripheries near or close to Cairo city to extend the occupational area and to release the socio economic stresses affecting Cairo due to overpopulation and development practices. The

*Corresponding author. E-mail: samykhalaf2005@yahoo.com.

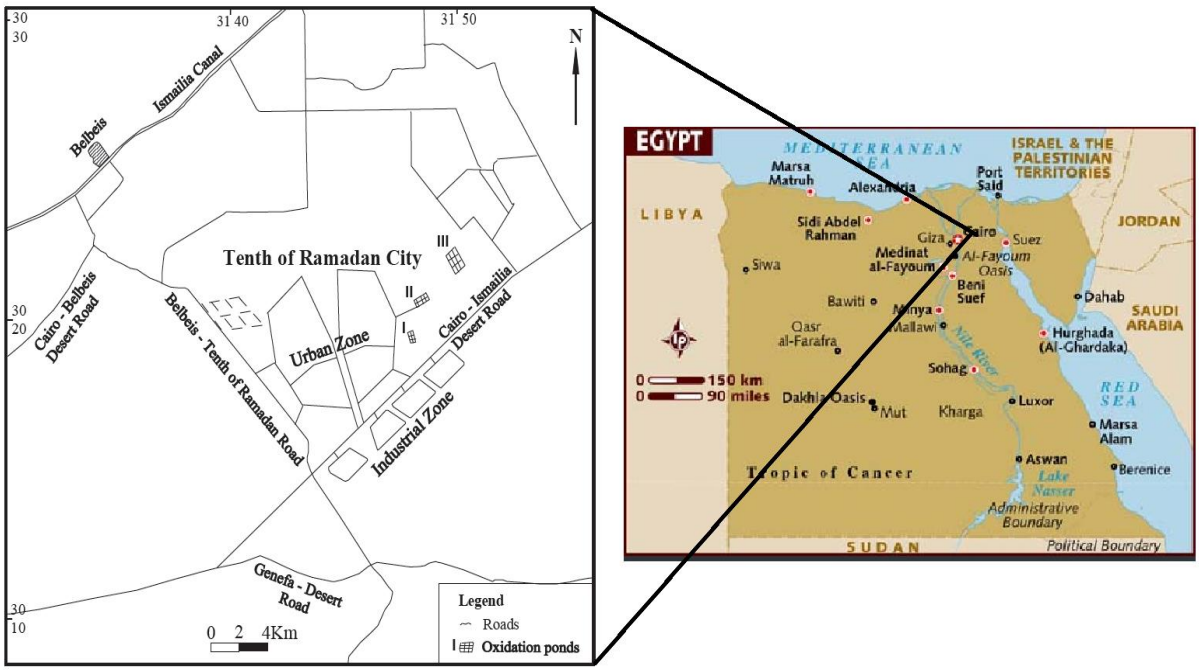

Figure 1. Location map of the study area

concerned city is located on the fringes of the eastern Nile delta region along Cairo–Ismailia desert road between longitudes 31°30'–32°00' E and latitude 30°00'–30°30'N, with area of about 465 km^2. It is bounded by Cairo-Belbies desert road from west, El Shabab canal from east, Ismailia canal from north and Cairo-Ismailia desert road from south. The study area as shown in Figure1 is characterized by desert climate with arid, hot and rainless summer, and mild winter with scarce amount of precipitation. Since, 1980 the domestic and industrial wastewater of the 10th of Ramadan city has been collected and disposed in three oxidation ponds. Overflow from these ponds is discharged into Wadi El-Watan about 15 km Northeast of the city by artificial and natural canals and is collected in low lands to treat El-Shabab fresh water canal. These accumulated effluents in the low lands are directly used for irrigation of new reclaimed areas. Oxidation pond No. 1 collects the effluent of domestic wastewater from the urban areas by a rate of 4000m^3/day (Table 1). Oxidation pond No. 2 collects domestic and part of the industrial wastewater with an average flow of about 13000m^3/day. Oxidation pond No. 3 collects the effluent from heavy industries at an average flow of about 25000m^3/day (Taha et al., 2004). These figures have changed over time.

GEOMORPHOLOGICAL AND GEOLOGICAL SETTINGS

The geomorphology and geology of the study area has been studied by many authors. Among them are Abbas (1953), Shukri (1953), Shukri and Ayouty (1956), Said and Beheri (1961), Soliman and Faris (1963), Shata (1965), El Fayoumy (1968), Shata and El Fayoumy (1970), Ahmed (1977), Kotb (1988), El Fawal and Shendi (1991), Ezz El Deen (1993). These previous studies covered all geomorphologic and geologic settings. Geomorphologic units in the study area include El Ankabia-Iweibid structural plain in the south, Bitter lakes and Isthmus plain in the east, Belbies- El Tell El Kabier-El Salhia plains (old deltaic plains) in the north, Wadi El Tumilat depression and Desert dry drainage lines (Figure 2-left). Ground elevation rises from 12 m amsl in the north, to about 180 m amsl in the south. The 10th of Ramadan city is located on the gravelly fluviatile plains. These plains occupy the area west of the cultivated lands of the Nile Delta and extend to Suez Canal.

The geology of the 10th of Ramadan city is composed of sedimentary rocks which belong to Tertiary and Quaternary periods (Figure 2-right). Oligocene sands and gravels are well exposed at Gebel El-Hamza and Gebel Um El-Qamar unconformably overly the Upper Eocene sediments. The outcrops of basaltic flows are observed at Gebel Um Raqm and El-Hamza. These basalts are unconformably underlying the marine Miocene sediments. The Pliocene sediments are recorded in the subsurface sections (up to 250 masl). These are composed of rarely fossiliferous dark pyritic clay. The Quaternary sediments cover a major part of the study area. The old wadi deposits of the terraces of the large wadis in the southern portion of the study area are

Table 1. Effluent discharges of oxidation ponds in the study area (RIGW, 1997).

Pond No.	Number of basins	Area (m^2)	Discharge (m^3/day)		Source (%)	
			March	April	Domestic	Industrial
1	6	400,000	22,000	18,000	46	54
2	6	400,000	20,000	27,000	19	81
3	9	500,000	25,000	24,000	5	95

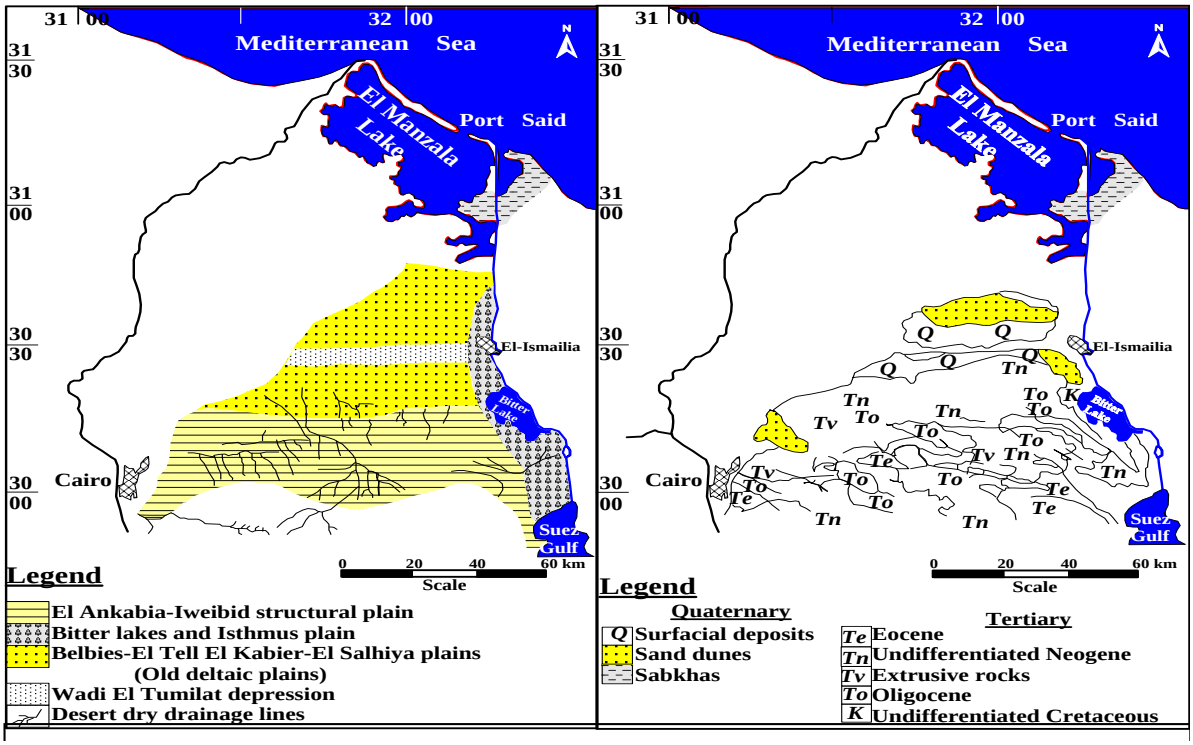

Figure 2. Geomorphological map (left) and geological map (right) after geological (right map) compiled after geological map of Egypt 1971.

formed of quartz sand, flint and quartzite pebbles.

HYDROGEOLOGICAL SETTINGS

The hydrogeologic framework of the study area is described based on the hydrogeological cross-section as shown in (Figure 3). The aquifers that have been encountered at the study area during the hydrogeologic investigations of the site include the Quaternary Aquifer of the 10th of Ramadan City Area (QARCA) and the Miocene aquifer (Figure 3). The current understanding of the configuration of the two aquifers and confining clay units shows neither of the two aquifers is continuous for the entire length of the study area, and both are interconnected in the southern central part of the study area where the groundwater is mixed. Although there is some interconnection between QARCA and Miocene aquifers, they have historically been treated as two separate aquifers (Sallouma, 1983; Gad et al., 2015). It is likely that groundwater flow in the QARCA and Miocene aquifers at the study area is local, and the flow paths are short (Figure 4).

The combination of the hydraulic barrier to the west, the localized recharge area, and the presence of large Ismailia canal, drains and eastern lakes and Sabkhas surrounding the study area effectively isolates QARCA in the central, northern and eastern parts from the influence of the regional groundwater flow system. The QARCA is unconfined and composed of fluviatile and fluvio-marine graded sand and gravel with clay intercalations of limited extension. It is mainly recharging by seepage from Ismailia canal and the other sub irrigation canals (El-Haddad, 2002; Embaby and El- Haddad 2007). Another local recharge is the infiltration from the oxidation ponds present in the study area The Miocene aquifer is dominated by clastic facies in the southern part of the study area and overlain by about 200 m of Quaternary deposits. This

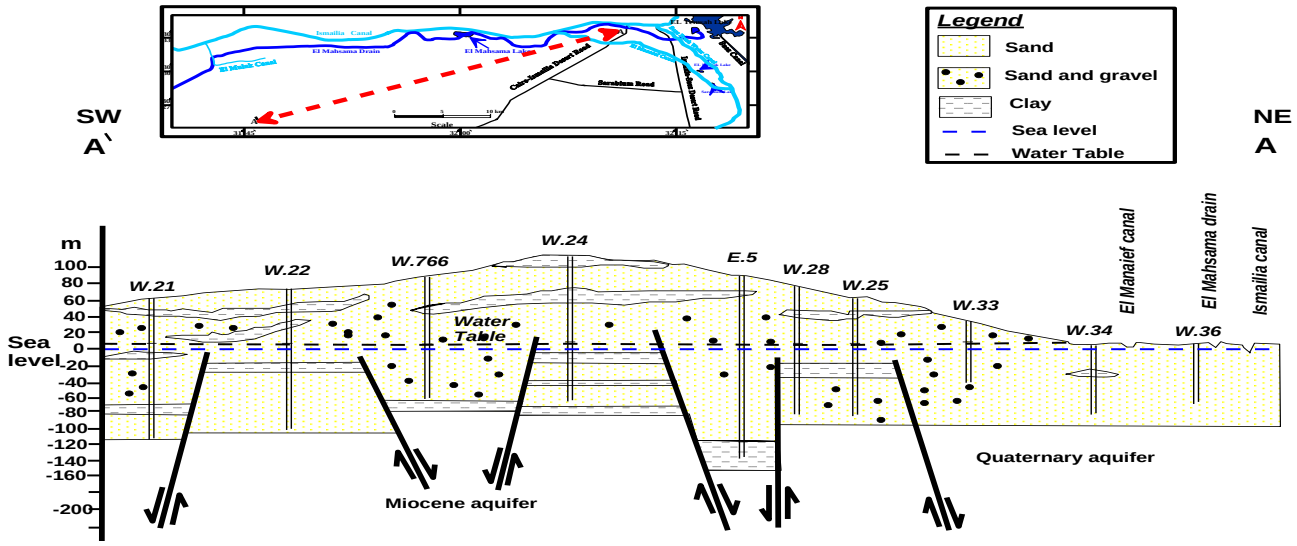

Figure 3. The cross-section along the QARCA monitoring well line in NE-SW direction showing different water bearing formations (after Gad, 1995).

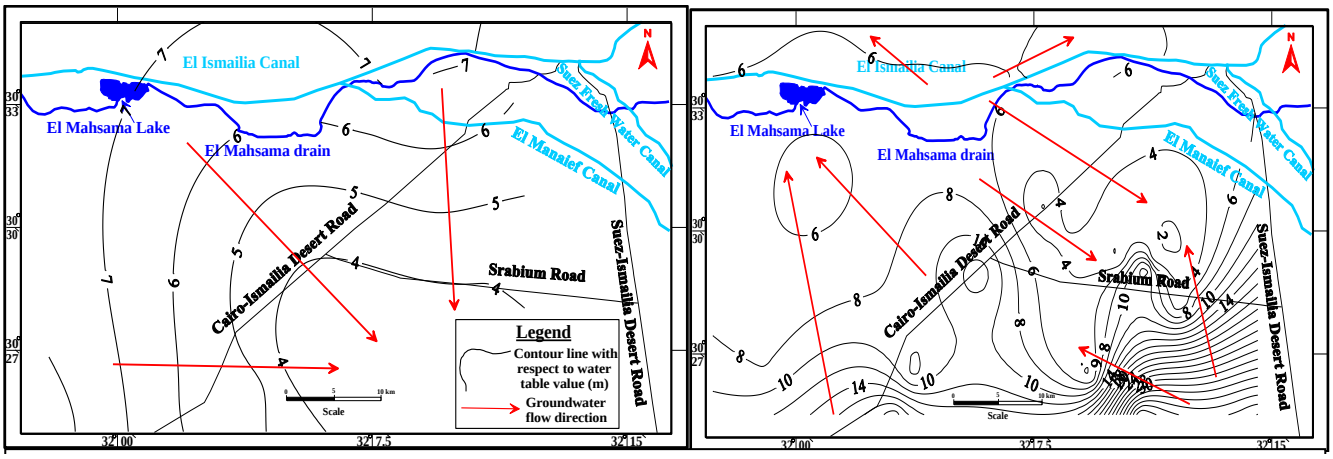

Figure 4. Water table contour map in Dec. 1992 (left, after Gad 1995) and in Dec. 2005 (right, after Ismail 2008)

great depth reflects less contamination than QARCA.

The objective of this research was to apply a groundwater model utilizing USGS MODFLOW coupled with solute transport engines to predict the transport and heavy metals contamination from the site.

MATERIALS AND METHODS

The numerical simulation of the groundwater flow and solute transport in the QARCA is mainly based on the results of the chemical analyses of 16 water samples collected from the wastewater of the oxidation ponds and groundwater wells in December 2010 and July 2012. Samples were collected usingstandard EPA methods and transported to the laboratory of the DRC. All collection procedures and analytical methods conform to U.S. EPA protocols (US EPA, 1996). The results besides the archival data from the previous works were collected in order to clarify the main different pollutants from industrial and agricultural activities. Heavy metals were determined using inductively coupled plasma (ICP) apparatus. The used analytical procedures of wastewater samples follow the methods adopted by Rainwater and Thatcher (1960).

The methodology used in this paper depends on the numerical simulation of groundwater flow and solute transport applying Visual MODFLOW software. Visual MODFLOW Premier, a Graphical User Interface (GUI) from Schlumberger Water Services Inc. that uses the USGS MODFLOW computer code was used to build a three-dimensional model of subsurface water flow. The governing equations of the groundwater flow are derived by mathematical combine between the water balance equation and Darcy's law (Anderson and Woessner, 1992). The model describes ground-

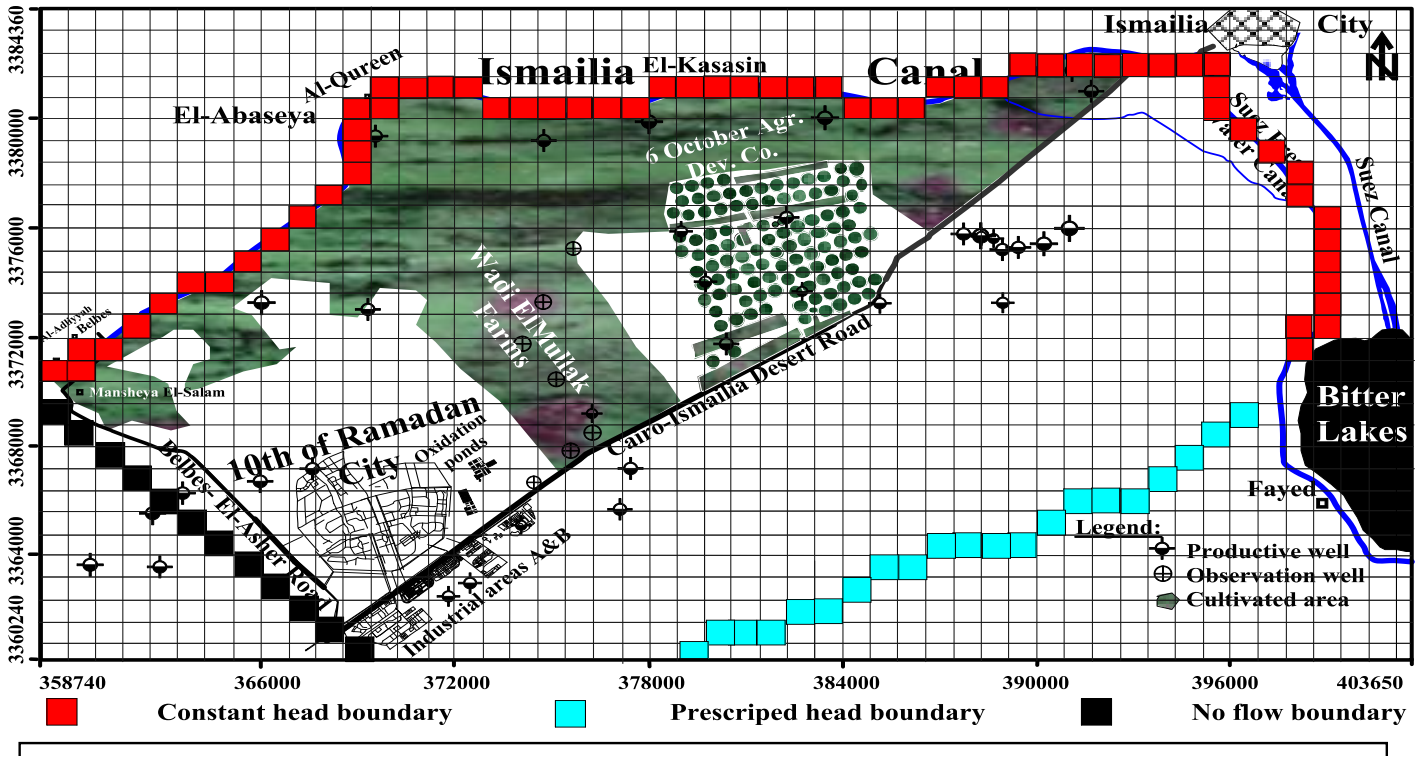

Figure 5. Finite difference grid and boundary conditions of model domain of QARCA.

water flow under non-equilibrium conditions in a heterogeneous and anisotropic medium according to the following equation (Bear, 1979; Bear and Verruijt, 1987):

$$\frac{\partial}{\partial x}\left(K_{xx}\frac{\partial h}{\partial x}\right)+\frac{\partial}{\partial y}\left(K_{yy}\frac{\partial h}{\partial y}\right)+\frac{\partial}{\partial z}\left(K_{zz}\frac{\partial h}{\partial z}\right)-W=S_s\frac{\partial h}{\partial t} \quad (1)$$

Where K_{xx}, K_{yy}, K_{zz} are values of hydraulic conductivity along the x, y and z coordinate axes (LT^{-1}); h is the piezometric head (L); W is a volumetric flux per unit volume and represents source and/or sinks of water (T^{-1}); S_s is the specific storage of the porous material (L^{-1}) and t is time (T).

The simulation procedure was started by dividing the QARCA domain into a grid pattern of 1500 cells (50 columns and 30 rows). The model cell area covered 1 km^2 and included area covers the three oxidation ponds and El-Mahsama Lake and different water bodies. The QARCA was assumed as one complex layer composed of sand and clay intercalations with lateral and vertical facies changes. It was surrounded by fixed head boundary from north (Ismailia canal), east (Suez fresh water canal), general head boundary from south, and no flow boundary from west. The top and the bottom of the aquifer layer and the boundary conditions were assigned to this grid (Figure 5). An annual recharge rate of 14 mm/year and an annual evapotranspiration rate of 2920 mm/year were applied to the model based local data (General Authority of Meteorological Stations, 2000). Oxidation ponds and El-Mahsama Lake were added as lake features, using depths provided by field measurements (3 m). The Ismailia canal was added as a river boundary using an average depth of 4 m (Gad et al., 2015). Both the lake and river boundary areas and shapes were input by tracing the features on the local digital quadrangle.

The surface layer of the model was based on the latest soil survey completed in 2008 (Table 2) by the Desert Research Center (Ismail, 2008). Topographical data were retrieved from the DEM file covered the modeled area with resolution 90mx90m and applied to the surface to show terrain (Figure 6). The second layer of the model was designed using values that were calculated from available well logs data. The conductivity was calculated from analysis of available pumping test using a piezometer following standard USGS accepted methods (Fetter, 1994). Porosity and bulk density were collected from Shata (1978). The elevation of the QARCA base was determined using the top layer elevation data and using SURFER to subtract 200m from it to represent the assumed thickness of the QARCA.

Values that were required for each layer included storativity, specific yield, conductivity, and porosity; they were calculated using equations of pumping test analysis beside available data (Table 3). MODFLOW was set to 18,250 days (50 years approximately) to represent the total time frame required for any sustainable development project.

In addition, simulation of soluble contamination migration by computer is a way to cover the hiatus between field observations and characteristics water movement in porous media. Computer Software can simulate the spatial variability of groundwater flow from one point to other points; it also shows interaction between surface and subsurface water. Along with such process it also possible to monitor and follow the contaminations which exist in groundwater or infiltrated from wastewater oxidation ponds by lateral and/or vertical migration.

As contamination moves it disperses. This means that the concentration decreases as it moves far then away from the source of the pollution. For this reason there is different concentration of contaminants at different points in the aquifer. The partial differential equation for three-dimensional of a reactive transport of contaminants in groundwater is given by (Freeze and Cherry 1979):

Table 2. Grain size and infiltration capacities of soil types in QARCA

Test No.	Infiltration rate(m/day)	Degree of Infiltration	Types of soli based on infiltration rate	Type of soli based on grain size analysis
1	1.72***	Moderately rapid	Good permeability sand	Gravelly sand soli
2	5.872***	Rapid	Sands and loamy sands	Loose sand soli
3	0.961***	Slow	Clays-clay loamy-sandy loam	Sandy loam soli
4	6.335***	Rapid	Sands and loamy sands	Loose sand soli
5	1.15*	Moderate	Clays-clay loamy-sand loamy	Clayey sand soli
6	6.03*	Rapid	Sands and loamy sands	Loose sand soli
7	1*	Moderate	Clays-clay loamy-sand loamy	Clayey sand soli
8	0.08*	Slow	Clays-heavy clays-partially cemented gravels	Sandy loam soli
9	4*	Moderate rapid	Good permeability sand	Gravelly sand soli
10	3.36*	Moderate rapid	Good permeability sand	Gravelly sand soli
11	1.31*	Moderate	Clayey sands-clay loams-sand clay loam	Gravelly sand soli
12	1.12*	Moderate	Clayey sands-clay loamy –sand clay loams	Clayey sand soli
13	6*	Rapid	Sands and loamy sands	Loose sand soli
14	1.93	Moderate rapid	Good permeability sand loams. Sandy clay loams. Sand clays	Gravelly sand soli
15	73.296**	Very rapid	Open gravel without soil	Very coarse and gravelly sand
16	9.072**	Vere rapid	Open gravel without soil	Very coarse and gravelly sand

*these date after (Gad. 1995).**: These data after (Afify.2004).**:These data after(Ismail 2008)

$$\frac{\partial}{\partial x}\left(D_x \frac{\partial C}{\partial x}\right) - \frac{\partial}{\partial x}\left(CV_x\right) - \frac{\partial}{\partial y}\left(CV_y\right) + \frac{q}{\theta}C + \sum_{k-1}^{N} R = \frac{\partial C}{\partial t} \quad (2)$$

Where, C is the concentration of contaminant dissolved respective Cartesian co-ordinate axis, D_{ij} is the hydrodynamic dispersion coefficient, V_i is the seepage or linear pore water velocity, q_s is the volumetric flux of water per unit volume of aquifer representing sources (positive) and sinks (negative), C_s is the concentration of the sources or the sinks, θ is the porosity of the porous medium and R_k is chemical reaction term.

Moreover, due to the hydrodynamic dispersion, the concentration of a solute will decrease over distance. Generally speaking, the solute will spread more in the direction of groundwater flow than in the direction normal to the groundwater flow, because longitudinal dispersivity is typically 10 times higher than transverse dispersivity. The transport of a conservative solute in a one-dimensional system can be described by the advection-dispersion equation:

$$\frac{\partial C}{\partial t} = -v\frac{\partial C}{\partial x} + D\frac{\partial 2C}{\partial x 2} \quad (3)$$

where:

∂C/∂t is the change in concentration over time, the first term on the right-hand side represents advection and the second term represents hydrodynamic dispersion. The advection-dispersion equation may be solved analytically or numerically under different initial and boundary conditions.

MT3DMS was used to predict heavy metal transport using lead as the surrogate. This engine is the best choice when biodegradation is not a factor when dealing with heavy metals that are persistent (Prommer et al., 2002). The adsorption coefficients were also most appropriate with the MT3DMS engine with heavy metal only having one oxidation state. Geochemical modeling of the Iron concentrations in PHREEQ C-2 indicated that very minimal trivalent iron (10^{-8} mol) would dissociate with the underlying reduced groundwater conditions in this area. Therefore, Iron was used as a surrogate. The initial concentration of Iron was based on the assumption of a constant leakage of 1 mg/L per day for 18,250 days (50 years). This was the estimate of constant leakage from the oxidation ponds since the first complaint in 1988 (Heiba, 1992). A Langmuir sorption curve was used with values calculated from sediment testing and previous studies on similar sediment types. Langmuir was used over Freundlich due to the losses from a single spill incident assumed to be two orders of a magnitude greater through the ground and a very little clay in the soils of the region minimizing additional sorption sites. The model was run using the hydraulic conductivity for the media as calculated as

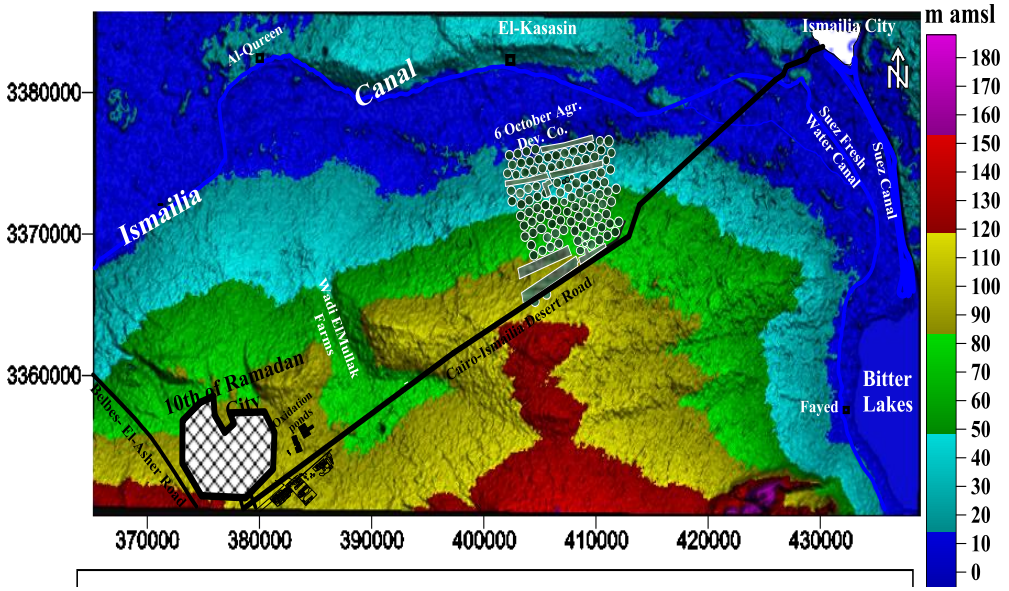

Figure 6. Ground elevation (m amsl) of QARCA extracted from DEM (Top layer).

Table 3. Hydraulic parameters of QARCA

Locality	Transmissivity (T) (m^2/day)	Storativity (S) (dimensionless)	Difusivity (m^2/day)
QARCA-Northern part	19986	0.0004	49965000
QARCA-Northern part	40600	0.0001	---------
QARCA-Northern part	20500	0.0001	---------
QARCA-Northern part	35600	0.0011	---------
QARCA-Middle part	5947	0.0084	707976.19
QARCA-Middle part	17858	0.0009	19842222
QARCA-Southern part	9381	0.0117	--------
QARCA-Southern part	4784	0.0025	1913600
QARCA-Eastern part	752	0.0003	2506666.7
QARCA-Eastern part	21600	0.0145	1489655.2
QARCA-Eastern part	32100	0.0208	1543269.2
QARCA-Eastern part	16000	0.0097	-------

follows: K= T/d = 5947/200 = 29.7 m/day horizontally (Table 3). Vertical conductivity was set to 1.72 m per day based on default vertical conductivity solutions from infiltration tests (Table 2) (Gad, 1995; Ismail, 2008; Gad et al., 2015). Changing of the conductivity, dispersivity, and adsorption coefficients were done for sensitivity analysis and to parameter adjustment. This process allowed the groundwater model to be delineated for the maximum, minimum, and most probable extent of the plume. The model was run for numerous iterations and outputs were recorded at different time intervals to show the size and extent of the heavy metal plume.

RESULTS AND DISCUSSION

The pH values of the wastewater samples range from 5.8 to 8.9 indicating slightly acidic to slightly alkaline water while most of the samples are turbid (Table 4). However, some samples are characterized by low turbidity with variable colors, so all these samples have been filtrated before carrying out chemical analysis. Based on the contents of trace elements, heavy metals, minor ions and acceptable contaminant levels, it is clear from Table 4 that the ions concentration of B^{2+}, Ba^{2+}, Cd^{2+}, Co^{2+},Cu^{2+} , Mn^{2+} and Zn^{2+} in all wastewater samples are below the acceptable levels of WHO standard. About 62.5% of the total samples are polluted with Al^{3+} and Fe^{2+} ions. These pollutants may attribute to the wastewater of industrial activities such as Iron and steel factory in 10^{th} of Ramadan city as a general. While, all wastewater samples are polluted with Cr^{2+}, Ni^{2+} and Sr^{2+}. The rest of the elements (Pb^{2+}, V^{2+} and Mo^{2+}) are below detection

Table 4. Results of chemical analysis of wastewater ponds in the study area

Pollutant	Recommend Max. Conc. (mg/l)	Location of analysis (December 2010) in mg/l				Location of analysis (July 2010) in mg/l			
		Inflow station	Outflow station	Pond No. 1	Pond No. 2	Pond No. 1	Pond No. 2	Pond No. 3	Pond No. 4
PH	----	6.8	8.9	6.4	6.4	6.7	6.8	5.8	7.6
E.C.	-----	1358	4230	1612	1563	1764	2108	3520	2748
TDS	-----	922	2299	1032	1000	1129	1383	2253	1766
Al	0.2	0.583	0.487	0.517	0.219	0.185	0.118	0.695	0.458
B	1	0.184	0.157	0.162	0.269	0.269	0.277	0.397	0.292
Ba	2.0	----	----	0.079	0.079	0.085	0.2545	---	1.338
Cd	0.005	----	----	0.0007	0.0007	0.0009	0.0006	---	0.0006
Co	<0.05	----	----	0.0034	0.0031	0.003	0.0009	---	0.001
Cr	0.01	0.044	0.043	0.074	0.07	0.034	0.038	0.048	0.058
Cu	<0.05	0.0123	<0.009	0.0241	0.0334	0.0109	<0.009	0.007	<0.009
Fe	0.3	2.263	1.136	0.552	0.215	0.118	0.147	1.670	4.337
Mn	0.2	0.105	0.065	0.092	0.095	0.067	0.109	0.114	0.205
Mo	0.05	<0.004	<0.004	<0.0008	<0.0008	<0.0008	<0.004	<0.0008	<0.004
Ni	0.01	0.045	0.0389	0.056	0.045	0.034	0.032	0.032	0.047
Pb	0.05	<0.006	<0.006	<0.004	<0.004	<0.004	<0.006	<0.004	<0.006
Sr	0.11	0.535	0.491	0.528	0.526	0.588	0.552	0.491	0.508
V	0.01-0.1	<0.01	<0.01	<0.01	<0.01	<0.01	<0.01	<0.01	<0.01
Zn	5	0.245	0.178	0.117	0.047	0.026	0.021	0.122	0.141

limits. This may be due to the precipitation of these elements from aeration in the oxidation ponds.

Moreover, the spatial variation in Al concentrations fluctuated from 0.118 (July 2012 pond No.2) to 0.458 mg/l (July 2012 pond No.3), in B concentrations fluctuated from 0.269 mg/l (July 2012 pond No.1) to 0.292 mg/l (July 2012 pond No.3), in Cr concentrations fluctuated from 0.034 mg/l (July 2012 pond No.1) to 0.0578 mg/l (July 2012 pond No.3) and from 0.118 mg/l (July 2012 pond No.1) to 4.357 mg/l (July 2012 pond No.3) for Fe concentrations. Total concentrations of Al, Cr, and Fe as high as 0.458, 0.0578 and 4.357 mg/l, respectively, were recorded in oxidation pond No.3, implying contaminated pond (allowable limits are 0.2, 0.05 and 0.3 mg/l, respectively). A comparison of the three oxidation ponds indicated that the wastewater of oxidation pond No.3 seemed to contain higher total Zn and Pb but lower Cu concentrations than those of wastewater of oxidation pond No.1 and No.2. In addition, the temporal variation in pollutant concentration in the wastewater of the present oxidation ponds (Figure 7) show significant annual fluctuations for all heavy metals concentration in the three ponds, but no specific trends could be identified. These spatial and temporal variations suggest that the scale and representativeness of sampling require careful planning, and a single sample might not give a satisfactory evaluation of the levels of heavy metal contamination in the three oxidation ponds ecosystems (El-Sayed et al., 2012).

It is important to note that the results of the chemical analysis of the groundwater samples show the presence of the same heavy metals contamination (Table 5). Also, most spatial groundwater contaminants trends within the studied samples appear to be the result of surface water contaminant migration more than rock-water interaction along distinct subsurface flow paths (Figure 8). It is concluded, from these discussions, that the concentration of Al, Fe and Sr is higher than that the acceptable limit according to WHO limits. So, the prediction of future concentration of these contaminants is required through applying numerical simulation of the contaminant transportation.

The results of the groundwater flow simulation process (Figure 9) reveal that the implementation impacts of the base case scenario have more or less serious impacts on the QARCA storage and consequently, contamination plume expansion. Figure 9-A shows the predicted hydraulic head after time of simulation of 5 years in the cultivated and reclaimed area's drilled wells applying the present development strategy. It is noticed from the figure that, under the exploitation strategy of 1000 m^3/day/well(current exploitation scenario), the total drawdown points to 0.2m, in the area adjacent to Ismailia canal as shown in the dashed black curved line characterize wells of groundwater table of 9.6 m (Figure 9-A). The decline in the predicted hydraulic head drawdown in the southern part of the QARCA compared with the other aquifer localities may be attributed to the increase in aquifer thickness and increase in sand ratio. Moreover, the decline in the hydraulic head will continue

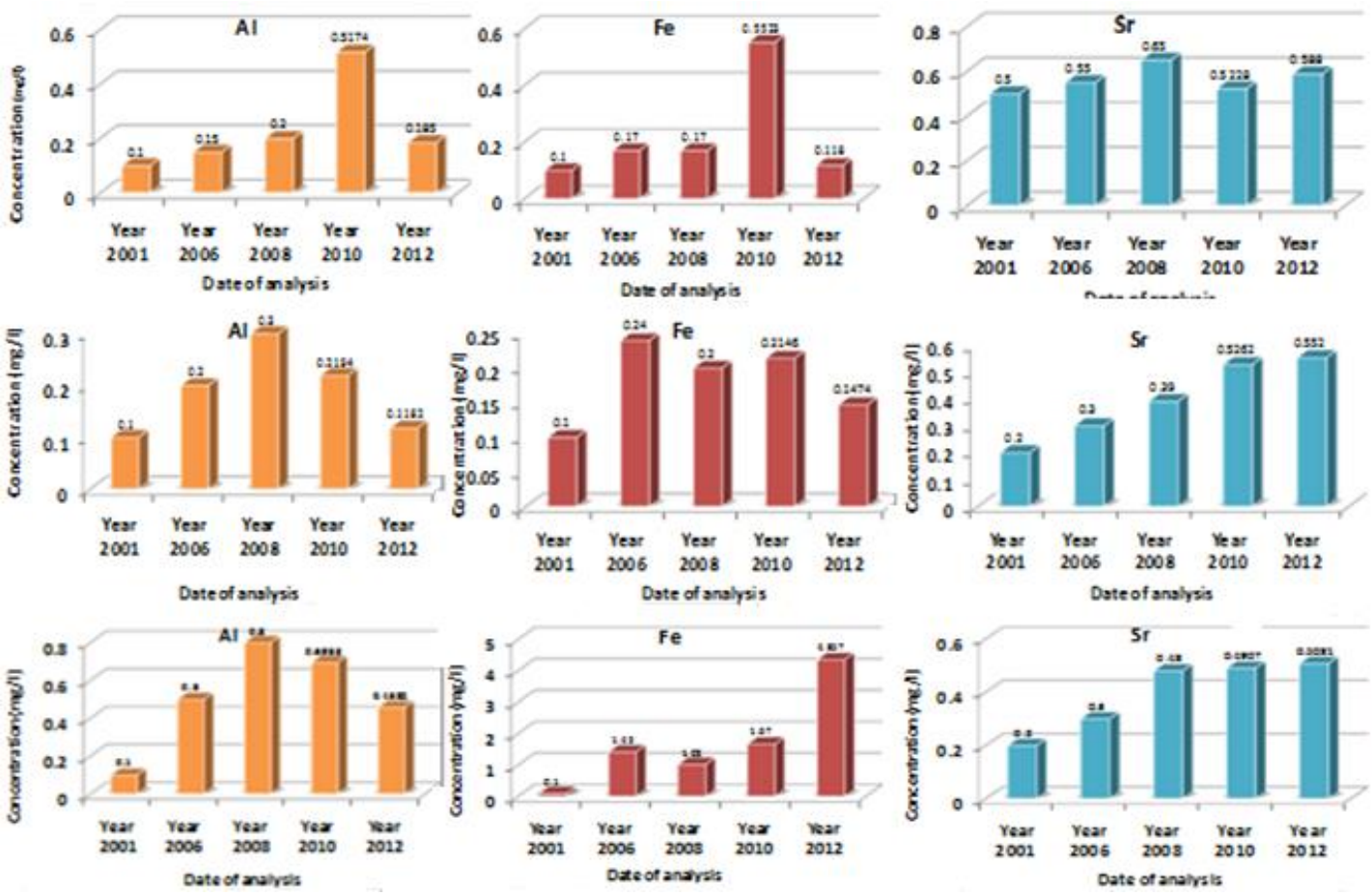

Figure 7. Temporal variations in Al, Fe and Sr concentrations in Oxidation pond No.1 (upper). Oxidation pond No.2 (middle) and Oxidation pond No.3 (lower).

till about 30 years of the simulation period of 50 years. After this interval, the groundwater system in the QARCA will be balanced. Moreover, the QARCA encompasses a large number of "flow domains" related to the appeared drawdown cone after simulation period of 20 years (Figure 9C), as the pump rate becomes more than the QARCA recharge. This condition will result in piezometeric head decline within the area followed by local groundwater flow from south, east and west directions towards the wells of the El Mullak cultivated area and 6 October for agricultural development company (Figure 9E). There are two cones of depression as a result of high discharge in the west and northeast direction and still increase after 10, 15, 20, 30 years but after 40 years there will be three high discharge zones (Figure 9F).

In addition, to discuss the relation between the changes of the predicted heads in the northeast direction with groundwater travel distance from the oxidation ponds during time of simulation of 50 years (Figure 10), it is concluded that when the distance increases the head decreases until it reaches its minimum value at distance of 28 km from the ponds and then return to increase. Also, when the time increases the head decreases, which reflects an expected increase in the contaminant plume expansion.

Aluminum, Iron and Strontium cannot leach and move with groundwater in the short time because of high absorption capacity of the soil for adsorption of Aluminum, Iron and Strontium particles (Khan and Ansari, 2005) but mobility of them are assumed as the adsorption capacity of the soil is reached. It should be noted that the periods of contaminants migration prediction were selected differently (5, 10, 15, 20, 30, 40 and 50 years) to obtain the distinctive results and approving mobility of overloaded Aluminum, Iron and Strontium within the longer time in the study area. This enables the groundwater carried contaminants to bypass the soil particles which permit transportation of high concentrations through the soil (Knapp, 2002; Saghravani and Mustapha, 2011).

From Figure 11 which represents the contaminants predicted movement in QARCA after 50 years of simulation, it is noticed that the contamination is migrating from the oxidation ponds. The source plume

Table 5. Results of chemical analysis of groundwater of QARCA

Parameter	Recommend Maxi. Conc. (Mg/l) (WHO 2004& 2011)	Henawy Farm (Sl)	Tony Farm (S2)	Km 70 (S3)	Km 63 (S4)	Amoon Farm (S5)	Mostafa Farm (S6)	Km60 (S7)	Km55 (S8)	Average
Date		Dec-10	Dec-10	Dec-10	Dec-10	Jul-12	Jul-12	Jul-12	Jul-12	
PH		7.6	6.5	6.1	6.2	7.1	6.9	6.9	7.1	6.8
E.C.		2400	4310	1035	6400	8280	10930	20060	7640	7631.875
TDS		1536	2785	6624	4096	5161	7035	12438	4774	5556.125
NO_3	11	38	54.2	100	76.4	21	52.4	46.5	58.1	55.825
PO_4	1	0.0825	0.2098	0.2935	0.1478	0.14	0.05	0.44	2.1	0.43295
AL	0.2	0.109	0.4756	0.6249	0.3232	0.03	0.0438	0.2776	0.8609	0.301875
B	1	0.4522	4.028	2.22	0.4837	0.6513	0.4722	0.4201	0.506	0.779188
Ba	2	0.061	0.0721	0.0469	0.0292	0.0785	0.4685	0.2088	0.0775	0.092813
Cd	0.003	<0.0007	<0.0007	<0.0007	<0.0007	<0.0006	<0.0006	<0.0006	<0.0006	BDL
Co	<0.05	<0.001	0.001	<0.001	<0.001	<0.0007	<0.0007	<0.0007	<0.0009	BDL
Cr	0.05	<0.01	0.0263	<0.01	<0.01	0.0215	<0.01	<0.01	<0.01	0.005975
Cu	1	<0.003	<0.003	0.0092	<0.0057	<0.009	<0.009	0.0332	0.0286	0.009588
Fe	0.3	0.0405	0.0486	0.1445	<0.0625	<0.02	<0.207	2.633	0.7488	0.481863
Mn	<0.1	<0.003	<0.003	0.0098	0.0065	<0.005	0.0322	0.0578	0.0864	0.024088
Mo	0.05	0.0019	<0.0008	<0.0008	<0.0008	<0.004	<0.004	<0.004	<0.004	BDL
Ni	0.01	<0.001	0.0021	<0.0038	0.0033	<0.001	<0.001	<0.001	<0.001	0.00115
Pb	0.01	0.0064	0.0071	<0.004	0.0054	<0.006	<0.006	<0.006	0.0144	0.004125
Sr	0.11	1.985	2.0309	40.06	5.94	4.696	10.14	20.36	7.721	7.901375
V	0.01	<0.01	<0.01	<0.01	<0.01	<0.01	<0.01	<0.01	<0.01	BDL
Zn	3	<0.001	<0.001	0.1338	0.0564	<0.0008	<0.0008	0.2085	0.1314	0.066263

appears to be a continuous source plume. The groundwater is moving towards wadi El-Mullak area and 6 October Agriculture Company. The contamination traveled at different distance as mentioned in Table 6. It will travel 18, 21 and 23 km due NE direction after 50 years of simulation for Al, Fe and Sr contaminant respectively. This means that the contaminant only travels at a speed of about 0.11m/day.

The areas affected by contamination are towards El Shabab canal, wadi El-Mullak area and 6 October Agriculture Company. In addition, there are lateral flow starts after 20 year which threatens a great part of the 10^{th} of Ramadan city.

CONCLUSION AND RECOMMENDATIONS

The wastewater from both industrial effluents and domestic sewage is drained into three incompletely lined oxidation ponds and directly used for irrigation of new reclaimed areas. The results show that the oxidation ponds are highly polluted by heavy metals such as Cr^{2+}, Ni^{2+}, Sr^{2+}, Fe^{2+} and Al^{2+}.

The infiltration from the oxidation ponds and expansion of reclaimed lands irrigated with wastewater reflect critical environmental hazards. The results of the groundwater flow and transport simulation reveal contamination plume expansion. It will travel 18, 21 and 23 km due NE direction after 50 years of simulation for Al, Fe and Sr contaminants respectively. It is highly recommended that wastes from oxidation pond must not be used in irrigation without treatment. New drilled wells should be located far away from pollution sources and observation wells should be installed around oxidation ponds for periodic monitoring.

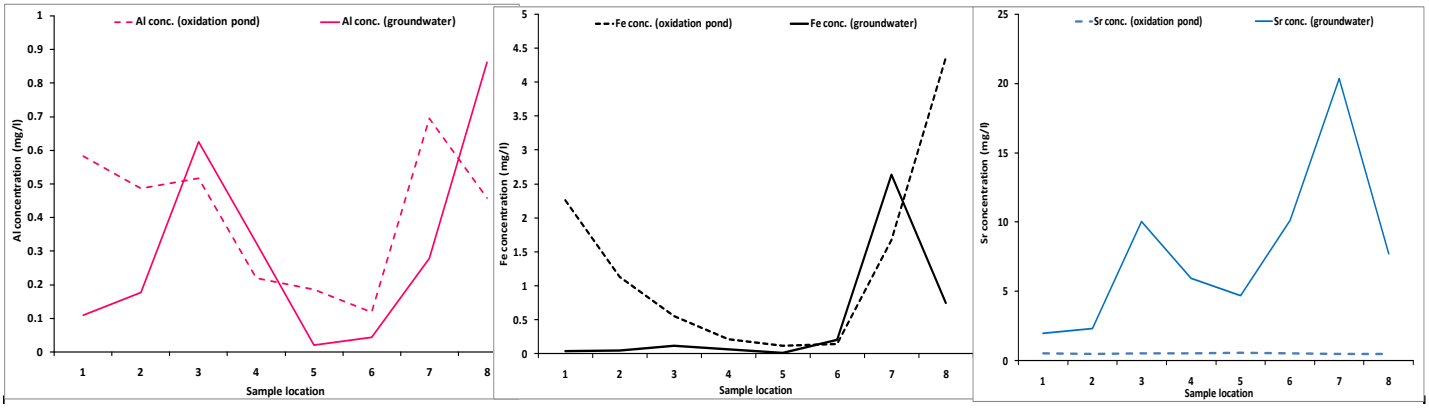

Figure 8. The general trend of Al contaminant (left), Fe contaminant (middle) and Sr contaminant (right) concentrations in groundwater and surface water samples in the study area

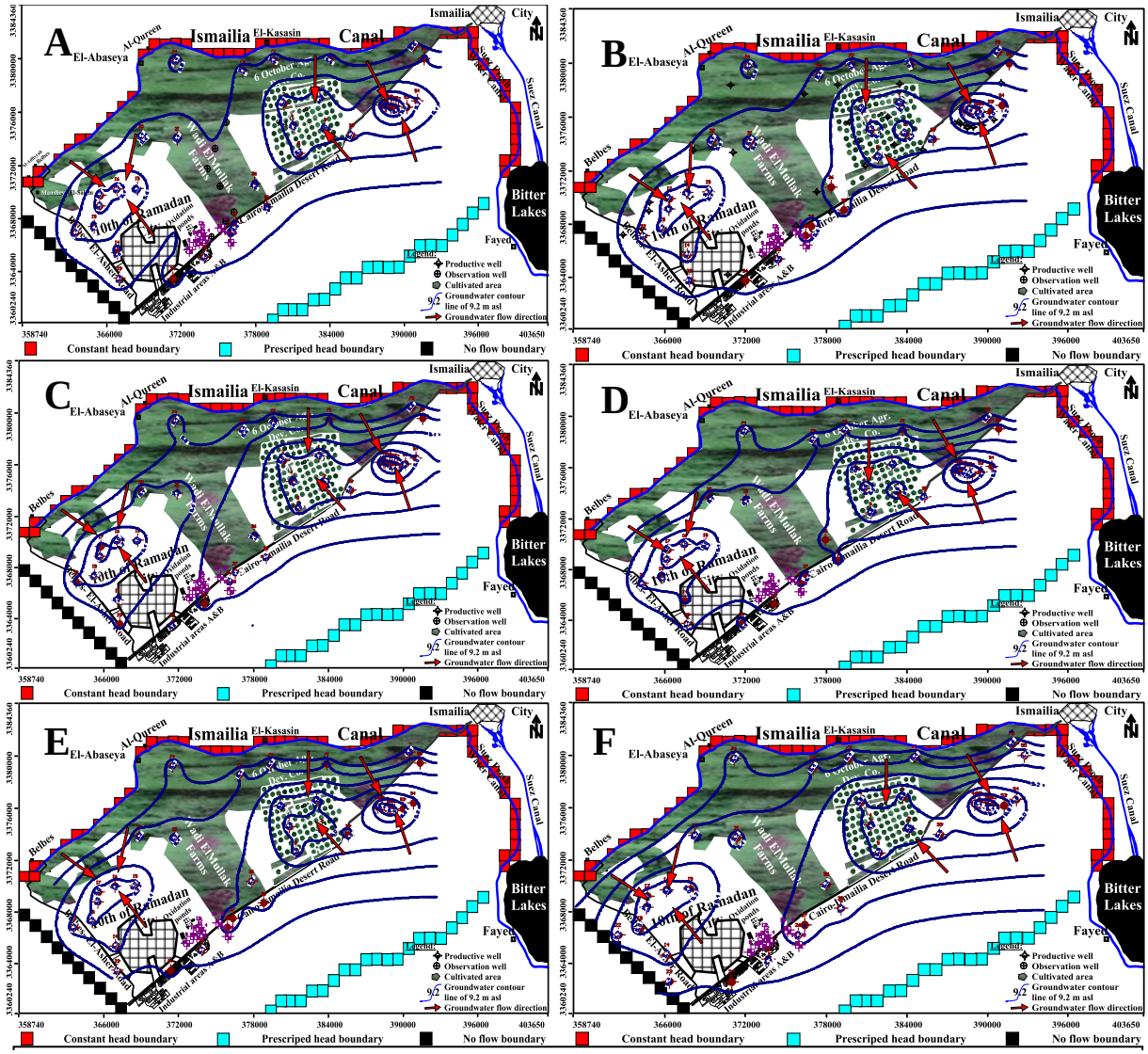

Figure 9. Predicted head of CARCA after simulation period of 5 years (A), 10 years (B), 20 years (C), 30 years (D), 40 years (E) and 50 years (F) in CARCA

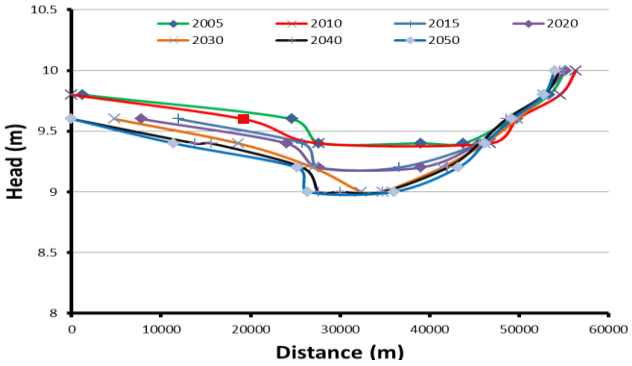

Figure 10. Predicted head vs distance from the oxidation ponds.

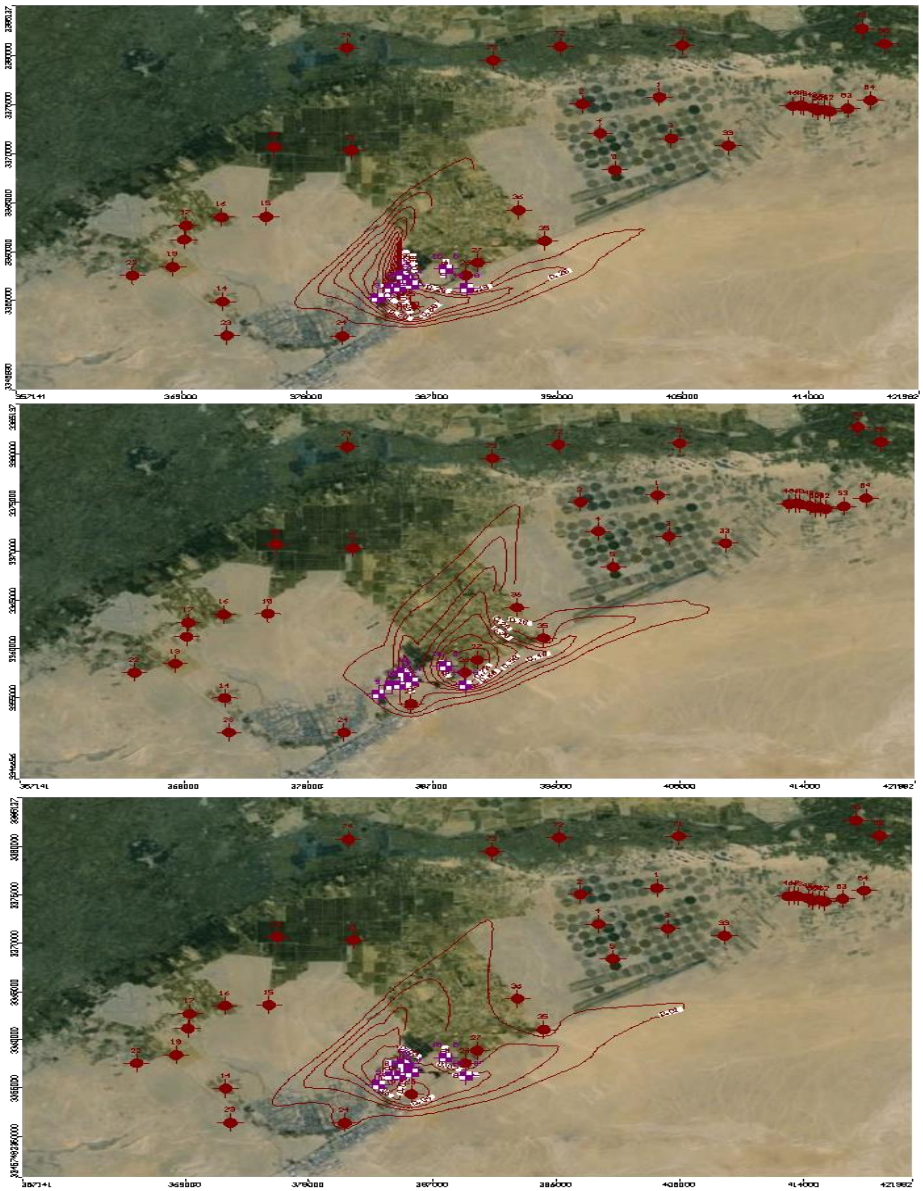

Figure 11. Predicted plume expansion after 50 years for Aluminum Al (upper), Iron Fe (middle) and Sr (lower).

Table 6. The expected contaminants plume migration distance from the source point (oxidation ponds) after time steps of simulation of 5, 10, 15, 20, 30, 40 and 50 years.

Pollutant Name	Plume migration in NE direction		Plume migration in SE direction	
	Time (year)	Distance (km)	Time (year)	Distance (km)
Al	After 5 years	15.3	After 5 years	13.5
	After 10 years	16.8	After 10 years	15
	After 15 years	17.4	After 15 years	16.5
	After 20 years	18	After 20 years	19.6
	After 30 years	18.6	After 30 years	22.8
	After 40 years	18.3	After 40 years	19.8
	After 50 years	18.1	After 50 years	22.5
Fe	After 5 years	16.5	After 5 years	15
	After 10 years	18	After 10 years	16.5
	After 15 years	19.5	After 15 years	18.3
	After 20 years	19.8	After 20 years	19.8
	After 30 years	20.4	After 30 years	22.2
	After 40 years	20.7	After 40 years	23.4
	After 50 years	21	After 50 years	24
Sr	After 5 years	18.3	After 5 years	16.5
	After 10 years	20.1	After 10 years	18.3
	After 15 years	21.3	After 15 years	19.2
	After 20 years	21.6	After 20 years	21.3
	After 30 years	22.5	After 30 years	24
	After 40 years	22.8	After 40 years	25.8
	After 50 years	23.4	After 50 years	27.6

Conflict of interests

The authors have not declared any conflict of interest.

REFERENCES

Abbas HL (1953). Contribution to the stratigraphy of the Mokattam Hill and its structure, Cairo, M. Sc. Thesis, Faculty of Sci. Alexandria university. pp.1-23.

Ahmed SA (1977). The geology of the desert east of Cairo. Bull. Inst. Desert Egypt 111:42-89.

Anderson MP, Woessner WW (1992). Applied groundwater modeling: Simulation of flow and Advection transport" Academic Press, San Diego, New York Boston. 318p.

Bear J (1979). Hydraulics of Groundwater. McGraw-Hill, New York.

Bear J, Verruijt A (1987). Modeling Groundwater Flow and Pollution. D. Reidel Publishing Company, Dordrecht, Holland. 414p.

El-Haddad IM (2002). Hydrogeological studies and their environmental impact on future management and sustainable development of the new communities and their surroundings, east of the Nile Delta, Egypt. Ph.D. Thesis, Faculty of Sci. Mansoura Univ. 435p.

El Fawal FM, Shendi EH (1991). Sedimentology and groundwater of the Quaternary sandy layer north of Wadi EI-Tumilat, Ismailia, Egypt. Ann. Geol. Surv. Egypt 17:305-314.

El Fayoumy IF (1968). Geology of groundwater supplies in the region east of the Nile Delta, Ph. D. Thesis, Faculty Sci. Cairo University 201p.

Embaby AA, El-Haddad IM (2007): Environmental impact of wastewater on soil and groundwater at the Tenth of Ramadan City area, Egypt. Mansoura J. Geol. Geophys. 34(2):25-56.

El-Sayed MH, El-Aassar AM, Abo El-Fadl MM, Abd El-Gawad AM (2012). Hydro-geochemistry and Pollution Problems in 10th of Ramadan City, East El-Delta, Egypt". J. Appl. Sci. Res. 8(4):1959-1972.

Ezz El Deen HM (1993). Sedimentological and geophysical studies of Heliopolis Basin, Cairo-Ismailia Desert Road and their applications, Egypt, M. Sc. Thesis, Faculty of Sci. Ain Shams University. 153p.

Fetter CW (1994). Applied Hydrogeology. New York, Macmillan, Englewood Cliffs, N.J. Prentice Hall. 691p.

Freeze RA, Cherry JA (1979). Groundwater, Prentice-Hall, Inc., Englewood Cliffs, New Jersey, U.S.A. 604p.

Gad MI (1995). Hydrogeological studies for groundwater reservoirs, east of Tenth of Ramadan City and vicinities. M. Sc. Thesis, Faculty of Sci. Ain Shams University Egypt. 187p.

Gad MI, El-Kammar MM, Ismail HMG (2015).Vulnerability Assessment of the Quaternary aquifer of Wadi El-Tumilat, East Delta, Using Different Overlay and Index Methods. Asian Rev. Environ. Earth Sci. 2(1):9-22.

Ismail HMG (2008). "Study the vulnerability of groundwater aquifer for pollution in Wadi El-Tumilat, Eastern Delta." Unpublished M.Sc. Thesis, Faculty of Sci. Cairo University. 286p.

Khan FA, Ansari AA (2005). Eutrophication: an ecological vision. The Bot. Rev. 71(4):449-482.

Knapp BJ (2002). Nitrogen and Phosphorus: Grolier Educational, ISBN-10: 0717275833; ISBN-13: 978-0717275830.

Kotb AM (1988). Geological, Hydrogeological and Geo-electrical studies on the eastern portion of Delta, M. Sc. Thesis, Faculty of Sci. Al Azhar University. 147p.

Prommer H, Barry DA, Davis GB (2002). Modeling of physical and reactive processes during biodegradation of a hydrocarbon plume

under transient groundwater flow conditions. J. Contam. Hydrol. 59(1-2):113-131.
Rainwater FR, Thatcher LL (1960). Methods for collection and analysis of water samples, V.S.G.S. water supply, paper No.1454, 301p.
RIGW (1997). Hydrogeological maps of Egypt scale 1:100,000. Water Research Center, Ministry of Public Works and Water Resources, Egypt.
Saghravani SR, Mustapha S (2011). Prediction of Contamination Migration in an Unconfined Aquifer with Visual MODFLOW: A Case Study. World Appl. Sci. J. 14(7):1102-1106.
Said R, Beheri S (1961). Quantitative geomorphology of the area east of Cairo, Bull. Soc. Geographic Egypt. pp. 121-132.
Sallouma MKM (1983). Hydrogeological and hydrogeochemical studies east of the Nile Delta, Egypt. Ph.D. Thesis, Fac. Sci. Ain Shams University. 166p.
Shata AA (1965). Geological structure of the Nile Delta. J. Eng. Cairo (in Arabic) pp. 1-3.
Shata AAA (1978). Genesis, formation and classification of the soils south Ismaelya canal between Belbeis and Ismaelya including Wadi El-Tumilat, M. Sc. Thesis, Faculty of Agric. Zagazig University. pp. 1-60.
Shata AA, El Fayoumy IF (1970). Remarks on the regional geological structure of the Nile Delta. Symp. Hydrol. Delta, UNESCO 1:189-197.
Shukri NM (1953). Geology of the desert area east of Cairo. Bull. Inst. Desert d' Egypte 3(2):89-105.
Shukri NM, El-Ayouti MK (1956). The Geology of Gebel Iwiebid, Gafra area, Cairo Suez District, Bull. Soc. Geogr. Egypt. pp. 67-71.
Soliman SM, Faris MI (1963). General geologic setting of the Nile Delta Province, 4th Arab Petrol. Congress, Beirut. pp. 19-28.
Taha AA, El-Mahmoudi AS, El-Haddad IM (2004). Pollution sources and related environmental impacts in the new communities southeast Nile Delta, Egypt. Emirates J. Eng. Res. 9(1):35-49.
US EPA. (1996). Standard Method 1669, Sampling Ambient Water for trace Metals at EPA Water Quality Criteria Levels.
World Health Organization standards for drinking water (WHO) (1996). International Standards for drinking water, Geneva Switzerland (3Ed):1, 130p.